Geodesic Holonomy Attractor between Surfaces of Different Curvature Signs relevant to Spin Transport

Bernd Binder[1]

Quanics
88679 Salem, Germany
(e-mail: `binder@quanics.com`)

Abstract. We will consider nonlinear holonomy effects -especially the spin dissipation dynamics- arising in the transport of a linear rotator between metric spaces with different curvature (positive, zero, negative). The extra 3D spin vector current induced by curvature and curvature change (measurable as precession) provides for a holonomic attractor called "Magic Angle Precession" (MAP) that could be relevant to 3D geodetic flows in classical mechanics, quantum physics, and quantum gravity based on chaotic dissipation. Limitations and instabilities of the spin current exchange are assigned to bifurcations at high precession loads as the driving gauge potential. In the classical range the chaotic dynamics can be verified with a mechanical toy gyroscope with built-in spin-precession coupling that could also be modeled by a Chua-type electronic circuit. Transporting vector currents composed by spin and precession is treated by Schwarz-Christoffel triangle maps with constant Schwarzian derivative and hypergeometric monodromy. In closed loops or periodic grids with alternating curvature the MAP attractor corresponds to a quantum state allowing for a lossless spin current transport without reflection. The Schrödinger hypergeometric quantum mechanical solution corresponds to Pöschl-Teller type equations with factorization and ladder operators. By pull-back we get the generalized Gauss linking number density differential form.
Keywords: holonomy, chaotic precession, geometric phase, hypergeometric, curvature, Berry, Chua, quantum gravity, Schrödinger, Pöschl - Teller, Legendre, Gegenbauer, Gauss, linking number, spin, magic angle spinning.

1 Introduction

We will compare rotators transported in hyberbolic, flat, and spherical spaces, where we get an extra 3D vector rotation induced by holonomy, a geodetic precession from parallel transport on curved paths. Rotated spin systems are very interesting from many different points of view. Adding a few extra coupling or damping terms, which is typical for a real system, can lead to chaotic precession (like a dissipation induced instability or bifurcation [6]), where it is rather expensive to actively control chaotic motion to obtain the sufficient stability conditions at the equilibrium points even for relatively simple gyroscope systems. Transporting rotatable rotators (gyroscopes [8]) likr spinning electrons over metric distortions in curved space or on curved

Bloch surfaces can result in a highly complex chaotic behavior due to non-linear holonomy effects in periodic loops [14]. In the classical limit we have no strong restrictions regarding the number and availability of states, but in the periodic or quantum case (standing holonomy waves) there are phase boundary conditions. In this paper we will provide for a general quantum transmission matching condition, previously called 'Magic Angle Precession" (MAP) supporting the transport of a linear rotator between metric spaces with different curvature [2]. We are looking for spin/precession preconditions given by or adjusted to a curvature step or metric distortions allowing for a lossless spin current with minimum reflection, where precession as a gauge field is driving the spin current.

2   Rotator Mediating or Parallel Transported between Surfaces with Different Curvature

Taking θ as the precession angle we assume that the rotator is parallel transported between surfaces with different curvature, where precession from holonomy can be classified according to the curvature sign (-1,0,+1) [9], [12]. Gyroscopic precession corresponds to the spherical case (subscript $_s$, curvature +1), Thomas precession (well known from special relativity) to the hyperbolic case (subscript $_h$, curvature -1). Both situation can be simultaneously treated by taking conformal mappings onto the flat Poincare disc (curvature 0), where we consider the real arc lengths given by the integrals $\theta_s = \int |d\theta_s|$ and $\theta_h = \int |d\theta_h|$ on the compact Riemann surfaces with conformal metrics

$$|d\theta_s| = \frac{2\,|d\xi_s|}{1 + |\xi_s|^2}, \quad |d\theta_h| = \frac{2\,|d\xi_h|}{1 - |\xi_h|^2} \; , \tag{1}$$

ξ_s or ξ_h are the complex variables on the Poincare disc, $r_s = |\xi_s|$ and $r_h = |\xi_h|$ are the radial distances, in spin dynamics often referred to as rapidity. From Poincare we know that we have the full group of isometries on this disc and also the sense preserving Möbius transformations $PSL(2, R)$ [13]. On the Poincare disc with a given center and scale we will first consider the arc length ratio between hyberbolic, flat, and spherical cases. With rotations measurable as precession exclusively induced by holonomy (which can be regarded as metric distortions [5], see below) we focus on the Möbius inversion between spherical and hyperbolic space as the fractional linear transformation connecting the conformal metrics in eq.(1). The correspondent distance inversion invariant can be written as a the differential product

$$d\theta_s d\theta_h = dr_s dr_h = 1, \tag{2}$$

where the arc length differential relation can be extended to an arc length integral length relation. Eqs.(2) and (1) are fullfilled by the rapidity relation

[2]

$$\frac{1}{1 - r_h^2} = \frac{r_s^2}{r_h^2} = 1 + r_s^2, \tag{3}$$

that provides for

$$r_h = \sin\theta_s = \tanh\theta_h, \tag{4}$$

and

$$r_s = \sinh\theta_h = \tan\theta_s. \tag{5}$$

With invariant arc lengths and length inversion $r_h r_s = \theta_h \theta_s$ providing for a
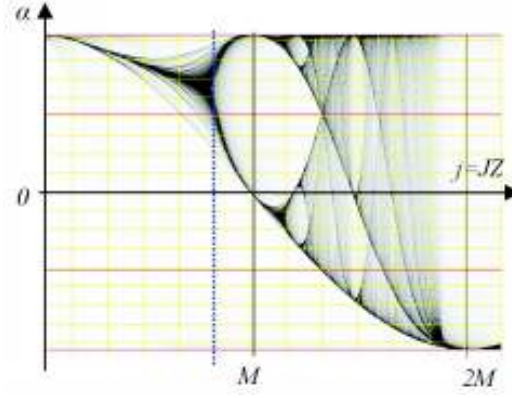

Fig. 1. MAP bifurcation diagram with $r_s = \pi j$ and $\theta = j\alpha$. Smearing effects are introduced due to phase fluctuations.

mapping condition, the measure characterizing the will be given by the ratio

$$f(\xi) = \frac{\int |d\xi_h|}{\int |d\theta_s|} = \frac{r_h}{\theta_s} = \frac{\int |d\theta_h|}{\int |d\xi_s|} = \frac{\theta_h}{r_s}. \tag{6}$$

Eqs.(4) - (6) provide for the θ_s and θ_h MAP conditions [4], [3]

$$\frac{r_h}{r_s} = \cos\theta_s = \frac{f\theta_s}{r_s}, \tag{7}$$

$$= \frac{1}{\cosh\theta_h} = \frac{f r_h}{\theta_h}. \tag{8}$$

f will represent coupling induced by a metric distortion leading to precession that can be expressed by a winding number M. For a given constant winding $f r_h \propto M$ in eqs.(7) and (8) (probably due to a periodic boundary or quantum condition) we are confronted with a chaotic attractor given by the cosine and hyperbolic cosine map [3] with bifurcation diagram shown in Figure 1.

3   Spin Triangulation and Hypergeometric Function

Spin and precession will have a triangular vector relation providing for the invariant total angular momentum on the tangential path of parallel transport. Changing curvature could be approached as a metric distortion f acting on triangular vector relation [2], [5]. We choose the situation where two out of three angles are identical ($A_s = A = A_h$, $B_s = B = B_h$), whereas the third angle $C_h < C < C_s$ is different due to holonomy or metric distortion, see Figure 2. Using wellknown expressions for the triangle functions considered
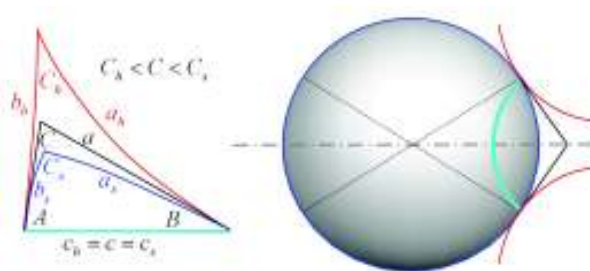

Fig. 2. The arc lengths of triangles of locally parallel curved surfaces (right) projected onto the Poincare disk (left). Hyperbolic is red, flat is black, spherical is blue with curvature $-1, 0, +1$, respectively. The triangles are locally aligned on the common arc $c_h = c = c_s$ (green), where two out of three angles are identical $A_s = A = A_h$, $B_s = B = B_h$.

here in terms of hypergeometric functions [13], the metric distortion can be written down more or less explicitly [5]. The metric distortion associated to a triangle map f is the ratio of the euclidean length element $|d\theta|$ at $\theta = f(z)$ to the spherical length element $2|dz|/(1 + |z|^2)$ at z, or to the hyperbolic length element $2|dz|/(1 - |z|^2)$ at z, depending on whether we have a spherical or hyperbolic triangle. This means, that the precession of the rotator in eq.(1) just measures the metric distortion. The algebraic solutions are given by the Gauss hypergeometric function $f(z) = {}_2\mathrm{F}_1\left(\begin{smallmatrix} a,\, b \\ c \end{smallmatrix} \middle| z\right)$ [5] obeying the hypergeometric differential (Fuchsian) equation

$$z(1-z)\frac{d^2 f(z)}{dz^2} + \left[c - (a + b + 1)z\right]\frac{df(z)}{dz} - abf(z) = 0. \qquad (9)$$

By the Riemann mapping theorem there is a conformal mapping sending the triangle vertices to the points $0, 1, \infty$, which are the singularities of hypergeometric ODE. The behavior of the hypergeometric (Gauss) equation (9) has three parameters a, b, c related to the singularities $\theta_1, \theta_2, \theta_3$ at $z =$

$\{p_1, p_2, p_3\}$ by

$$\begin{aligned}
\theta_1 &= 1 - c, \\
\theta_2 &= c - a - b, \\
\theta_3 &= a - b.
\end{aligned} \tag{10}$$

The general context of Hypergeometric functions can be applied to solve ordinary differential equations by symbolic computing of the Fuchsian form [1]

$$f'' + p(\alpha)f' + qf = 0, \quad \frac{df}{d\alpha} = f', \ \frac{d^2}{d\alpha^2} = f'', \ q = -ab = \pm\omega_q^2, \ q' = 0, \tag{11}$$

with $p, q \in \mathbf{C}(\alpha)$. As a simple test, we get the MAP functions eqs.(7) and (8) with $\alpha_s = \theta_s/2$ and $\alpha_h = \theta_h/2$

$$f_h = \propto \frac{M\alpha_h}{\cosh\alpha_h}, \ p_h = \tanh\alpha_h, \quad f_s \propto \frac{\cos\alpha_s}{M\alpha_s}, \ p_s = \frac{2}{\alpha_s}. \tag{12}$$

4   The Schwarzian Derivative

Possible $p, q \in \mathbf{C}(\alpha)$ can be obtained from the Schwarz criterion [13]. Let $s \in \mathbf{C}(\alpha)$ denote a quotient of two distinct solutions of the hypergeometric (Gauss) equation (9) and call it a *Schwarz map* for the hypergeometric equation, then one important criteria given by the *Schwarzian derivative* [5]

$$\{s, \alpha\} = \left(\frac{s''}{s'}\right)' - \frac{1}{2}\left(\frac{s''}{s'}\right)^2 = \frac{s'''}{s'} - \frac{3}{2}\left(\frac{s''}{s'}\right)^2 = 2q - p' - \frac{1}{2}p^2, \tag{13}$$

which is invariant under all linear fractional transformations, where all closed paths with a common fixed point give a group of fractional-linear transformations that acts on the branches of s generating the metric (1). The Schwarzian derivative is a criterion for the existence and monodromy of a compact Riemannian metric of constant curvature and a criterion for a proper pull-back transformation. With constant singularities $\theta_j' = 0$ we have with $q' = 0$ from eq.(13)

$$\{s, \alpha\}' = -p'' - \frac{1}{2}(p^2)' = 0, \ p = -\frac{p''}{p'}. \tag{14}$$

leading to

$$p \propto \tan(\omega_q\alpha), \ p \propto \cot(\omega_q\alpha), \ p \propto \tanh(\omega_q\alpha), \ p \propto \coth(\omega_q\alpha),$$
$$p \propto 2/\alpha. \tag{15}$$

From the metrics (1) with $r = |\xi|$ we get the real transcendental pull-back relations

$$z_s = \frac{1}{1 + r_s^2} = \frac{1 + t_s}{2} = \frac{1}{z_h}, \quad z_h = \frac{1}{1 - r_h^2} = \frac{1 + t_h}{2}, \tag{16}$$

$\xi = f(z)$	$p(\alpha)$	pullback z	a	b	c	context
$(\pi - \alpha)/\cos(\omega_q\alpha)$	$-2\lambda\tan(\omega_q\alpha)$	$(1+t)/2$	$\lambda \pm \epsilon$	$\lambda \mp \epsilon$	$\frac{1}{2}+\lambda$	MAP
$(\pi - \alpha)/\sin(\omega_q\alpha)$	$2\lambda\cot(\omega_q\alpha)$	$(1-t)/2$	$\lambda \pm \epsilon$	$\lambda \mp \epsilon$	$\frac{1}{2}+\lambda$	Linking Number
$(\pi - \alpha)/\cos(\omega_q\alpha)$	$-2\lambda\tan(\omega_q\alpha)$	$(1-t)/2$	$\lambda \pm \epsilon$	$\lambda \mp \epsilon$	$\frac{1}{2}$	MAP
$(\pi - \alpha)/\sin(\omega_q\alpha)$	$2\lambda\cot(\omega_q\alpha)$	$(1+t)/2$	$\lambda \pm \epsilon$	$\lambda \mp \epsilon$	$\frac{1}{2}$	Linking Number
$(\pi - \alpha)/\cosh(\omega_q\alpha)$	$2\lambda\tanh(\omega_q\alpha)$	$(1+t)/2$	$\lambda \pm \epsilon$	$\lambda \mp \epsilon$	$\frac{1}{2}+\lambda$	MAP
$(\pi - \alpha)/\sinh(\omega_q\alpha)$	$2\lambda\coth(\omega_q\alpha)$	$(1-t)/2$	$\lambda \pm \epsilon$	$\lambda \mp \epsilon$	$\frac{1}{2}+\lambda$	Linking Number
$(\pi - \alpha)/\cosh(\omega_q\alpha)$	$2\lambda\tanh(\omega_q\alpha)$	$(1-t)/2$	$\lambda \pm \epsilon$	$\lambda \mp \epsilon$	$\frac{1}{2}$	MAP
$(\pi - \alpha)/\sinh(\omega_q\alpha)$	$2\lambda\coth(\omega_q\alpha)$	$(1+t)/2$	$\lambda \pm \epsilon$	$\lambda \mp \epsilon$	$\frac{1}{2}$	Linking Number

Table 1. A table listing the hypergeometric solutions to $\xi'' + p(\alpha)\xi' + q\xi = 0$ with $\theta = 2\omega_q\alpha$, $q = -\omega_q^2 = \epsilon^2 - \lambda^2$, $t = \cos\theta$.

providing for the transcendental mappings

$$t_s = \cos\theta_s, \ t_h = \cosh\theta_h. \tag{17}$$

From now on we ommit subscript $_h$ and $_s$, which can be directly found from the hyperbolic or spherical type of the ODE2, see [1] and the list in Table 1.

5   Schrödinger Quantization and Factorization

We assume that the MAP solutions in eq.(12) are based on a conformal condition handling integral winding numbers on surfaces of constant curvature. Our monodromy-invariant metric description can be extended to paths of multiple integral extra loops which correspond in physics to quantum numbers and conditions. In one of his celebrated papers [10] Schrödinger took exactly one of the hypergeometric pull-back function we found applying the Schwarz criteria in equation (14) and showed how to factorize with this transcendental transformation the Gauss hypergeometric ODE2. He was aware that most of the interesting functions occurring in physics are either special or limiting cases of Gauss's function and indicated with $z \mapsto \phi(\theta) = \cos^2(\theta/2) = \cos^2(\omega_q\alpha)$ a quadruple of factorizations of the hypergeometric equation. In his transformation $t = \cos\theta = 2\phi - 1$ it was important that $0 \le \phi \le 1$ and that the independent variable θ is restricted to $\pi \ge \theta \ge 0$. He then found that

$$\frac{d^2 f}{d\theta^2} + \left(\frac{\omega_1\cos\theta + \omega_2}{\sin\theta}\right)\frac{df}{d\theta} + \omega_q^2 f = 0,$$

is factorizable and related to the hypergeometric solution

$$\omega_1 = a + b, \qquad \omega_2 = a + b + 1 - 2c, \qquad \omega_q^2 = -ab,$$

which provides for a direct route to the Schrödinger equation and associated potential with quantization, factorization and corresponding ladder operators

[1], [13], [10]. With $\omega_1 = \pm\omega_2$, $\sin\theta = 2\sin(\theta/2)\cos(\theta/2)$, and $\theta = 2\omega_q\alpha$ our spherical solutions with $q = \omega_q^2 = \epsilon^2 - \lambda^2 < 0$ correspond to the Gegenbauer polynomials $\xi(t) = C_n^\lambda(t) = C_{\pm\epsilon-\lambda}^\lambda(t)$, (see [1]), with associated Legendre polynomials $P_\nu^\mu(t)$ (spherical harmonics) where $\mu = \frac{1}{2} - \lambda$, $\nu = \pm\epsilon + \frac{1}{2}$, $n = \nu + \mu - 1$ leading to the Schrödinger equation of MAP on the disk

$$\frac{d^2\Psi_\nu^\mu(\theta_h)}{d\theta_h^2} + \left[\frac{D}{\cosh^2\theta_h} - \mu^2\right]\Psi_\nu^\mu(\theta_h) = 0, \tag{18}$$

where μ^2 is the energy eigenvalue. The Pöschl-Teller (PT) type potential

$$V(\theta_h) = -\frac{D}{\cosh^2\theta_h} \tag{19}$$

has potential depth $D = \nu(\nu + 1)$. There is an explicit connection of the PT potential with the $su(1,1)$ and $su(2)$ algebra describing the bending of coordinates in molecules, where θ_h gives the relative deviation from the equilibrium position.

6   Generalized Gauss Linking Number Concept

The quantification of the loop current is how to count the Writhe that is equal to the Linking minus the Twist. The Writhe can be assigned to the Gauss linking integral, the twist to the integral number of extra loops. Historically, the Gauss linking concept was limited to flat space but has been recently extended to higher-dimensional spherically curved surfaces, which provides for a generalized (curved) electromagnetism, Biot-Savart law, and Maxwell's equations (DeTurck and Gluck, Kupferberg [7]). It is easy to see, that the Gauss linking differential form generalized to higher-dimensional curved surfaces fits perfectly to our Fuchsian differential form and provides with the proper pull-back for the same solutions. According to Kupferberg [7], if the $SO(a, b)$-invariant differential form

$$\omega = \phi(t)\boldsymbol{x} \wedge \boldsymbol{y} \wedge d\boldsymbol{x}^{\wedge a-1} \wedge d\boldsymbol{y}^{\wedge b-1}, \quad t = \boldsymbol{x} \cdot \boldsymbol{y}, \tag{20}$$

on $H^+ \times H^-$ in $\mathbf{R}^{(a,b)}$ has $d_y d_x \omega = 0$, it satisfies the ordinary differential equation (11) with p-functions according to Table 1, e.g., for $f(\alpha) = \phi[t(\alpha)]$ with pull-back $t = \sinh\alpha$ and $p = (a + b)\tanh\alpha$ the corresponding ODE's are given by

$$f'' + (a + b)(\tanh\alpha)f' + abf = 0,$$

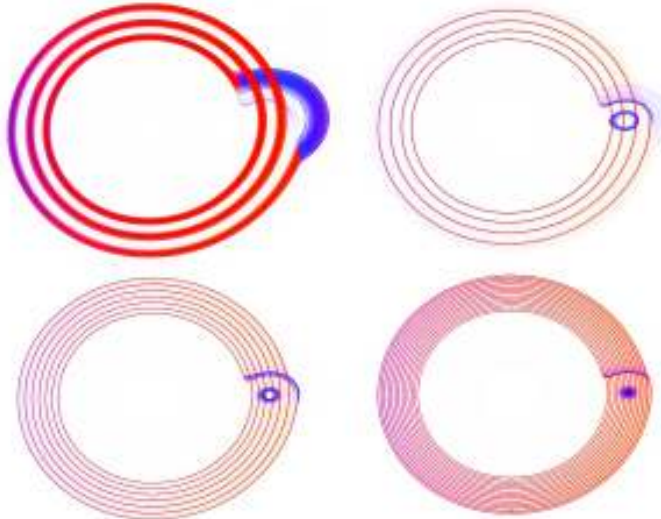$$(\cosh\alpha)^2\phi'' + (a + b + 1)(\sinh\alpha)\phi' + ab\phi = 0.$$

Fig. 3. A Chua-type model for chaotic quantum transitions, where a local singularity triggers the dissipation of a spin quantum characterized by a winding number load for $j = M$. On the top left we have $k/M = 2$, on the top right we have $k/M = 3$, on the bottom left we have $k/M = 5$, on the bottom right we have $k/M = 8$. The blue color indicates the influence of the holonomic coupling term $\cos[j(y - z)]$.

7   Quantum Chaotic Transitions

We are not only interested in the MAP condition but also in the dynamics of bifurcations or limit cycles given by the cosine map, see Figure 1. The hypergeometric ODE2 solutions to model the chaotic spin exchange via precession could be extended to distortion by local coupling singularities. In physics MAP can represents a special chaotic behavior in the precession angle if the rotor angular velocity is linearly coupled by (an)holonomy to the precession angular velocity and angle [4]. With metric distortion proportional to precession (precession angular velocity in a transport process), and precession proportional to spin, energy proportional to spin would recurrently conform Einstein's proposal that energy is proportional to a metric distortion. The linear coupling provides for conic paths and allows spinning up and controlling the rotor simply by forcing precession at special quantum magic precession angles. To approximate this behavior with monopole coupling strength $M\theta$ and nonlinear holonomic control function $\pi \cos[j(y - z)]$ from gyroscopic precession, we refer to a well known and rather simple system of coupled differential equations [3], where the geodesic flow of the attractor can be simulated and conceptually approached by a Chua-type system [11],

a well known and real-world model of chaotic dynamics given by

$$\frac{dz}{dt} = M(y - z) - \pi \cos[j(y - z)] \ ,$$

$$\frac{dy}{dt} = x - M(y - z) \ ,$$

$$\frac{dx}{dt} = -y + \frac{x}{k} \ . \tag{21}$$

Depending on the source strength $1/k$ of the driving oscillator and the number of phase singularities given by j/M, MAP shows a characteristic quantum spin dissipation dynamics given by a kind of winding ratio k/M, which is coupling strength $\propto 1/M$ divided by source strength $1/k$. For $j = M$ the phase space dynamics is shown in Figure 3. The differential equation system eqs.(21) describe chaotic currents, where the nonlinear impedance in Chua's original electronic circuit controlling the linear oscillator is a transcendental function $f(z) = \pi \cos[j(y - z)]$, the holonomic coupling term given by the total phase minus the Berry geometric phase [4],[3]. MAP can be found in the z-singularity $dz/dt = 0$ with $\theta = y - z$ and $r_s = \pi j$ and $\theta = j\alpha$, which can be approached and illustrated if we take the precession angle θ as the gauge potential term (showing Coulomb type "charge" and dipole effects) and the rotor spin as the electric current. Both systems have 3 degrees of freedom (two voltage y, z, one current x) and 3 energy storage elements (two capacitors and one inductivity as the rotor angular momentum setting the timescale), see [3]. In both cases a linear oscillator (precession in MAP) is coupled to a nonlinear element (holonomy in MAP). The nonlinear element responsible for chaos and bifurcation is driven by precession, where the geometric coupling current is delivered by the conductivity term providing for j missing or extra loops. The geometric phase induced by the curved path of the rotor or external curvature and part of the coupling increases with precession angle. Limitations and instabilities of the spin current exchange can be assigned to geometric phase bifurcations at high precession loads as the driving gauge potential.

8   Conclusions

MAP attracting a linear quantum state corresponds to a fixed winding number ratio characterized by closed loop or standing waves and corresponds to the situation, where spin currents remain intact while crossing the contact boundaries between regions of different curvature. This behavior can be simulated by Chua-type circuit models, where oscillator or spin currents are nonlinearly and recurrently coupled by holonomic precession, which is the driving gauge potential. This provides at strong coupling for a chaotic linking number density function, which has fixed points, limit cycles, and bifurcations. It should be noted that the chaotic dynamics can be verified

with a mechanical toy gyroscope having an in-build linear coupling between spin and precession [3]. In spatially periodic or loop situations we get a recurrent holonomy effect. In measurement the corresponding geometric phase effects can be found as precession angles or relative phase shift with respect to a reference beam in an interference experiment. Interesting applications for this new approach can be found in atoms or solids providing for closed loops or a spatially periodic holonomy. This finding could be relevant to the understanding of lossless (no radiation) nuclear, atomic, solid state quantum transitions, and large scale gravitational anomalies.

References

1. M. Abramowitz and I. A. Stegun. *Handbook of Mathematical Functions with Formulas, Graphs, and Mathematical Tables*. Dover, New York, 1972.
2. B. Binder. Holonomy attractor connecting spaces of different curvature responsible for 'anomalies'. In G. Robertson, editor, *SPACE, PROPULSION AND ENERGY SCIENCES INTERNATIONAL FORUM: SPESIF-2009*, volume 1103, pages 629–655, American Institute of Physics, 2008. AIP Conference Proceedings.
3. B. Binder. Magic angle chaotic precession. In Ch. Skiadas C. H. Skiadas, L. Dimotikalis, editor, *Topics on Chaotic Systems, Selected Papers from CHAOS 2008 International Conference*, volume 000, page 000, Singapore, 2008. World Scientific Publishing Company.
4. B. Binder. Magic angle precession. In M. El-Genk, editor, *Space Technology and Applications International Forum (STAIF-08)*, volume 969, pages 1103–1110, American Institute of Physics, 2008. AIP Conference Proceedings.
5. M. Bonk and W. Cherry. Metric distortion and triangle maps. *Annales Academi Scientiarum Fennic Mathematica*, 24:489–510, 1999.
6. H. K. Chen. Chaos and chaos synchronization. *J. Sound Vib*, 255(4):719–740, 2002.
7. G. Kupferberg. From the mahler conjecture to gauss linking integrals. *Geometric And Functional Analysis*, 18:870–892, 2008.
8. W. F. Osgood. *Mechanics*. MacMillan, New York, 1937.
9. A. J Rhodes and M. D. Semon. Relativistic velocity space, wigner rotation, and thomas precession. *Am. J. Phys.*, 72(7):943–960, 2004.
10. E. Schroedinger. The factorization of the hypergeometric equation. *Proceedings of the Royal Irish Academy*, 47 A:39–52, 1941.
11. L.O. Chua T. Matsumoto and M. Kumoro. The double scroll. *IEEE Transaction on Circuits and Systems*, CAS-32(8):798–818, 1985.
12. H. Yamasaki. Geometrical interpretation for relativistic composition of velocities and the thomas precession. *Europ. Journ. of Phys.*, 12(5):218, 1991.
13. M. Yoshida. *Hypergeometric Functions, My Love: Modular Interpretations of Configuration Spaces*. Vieweg, Braunschweig, 1997.
14. J. Zwanziger. *The Geometric Phase in Quantum Systems: Foundations, Mathematical Concepts, and Applications in Molecular and Condensed Matter Physics*. Springer, New York, 2003.